Monte Carlo Based Real-Time Shape Analysis in Volumes

Krishna Gurijala
Stony Brook University
New York, USA
gkrishna@cs.stonybrook.edu

Lei Wang
Stony Brook University
New York, USA
leiwang1@cs.stonybrook.edu

Arie Kaufman
Stony Brook University
New York, USA
ari@cs.stonybrook.edu

ABSTRACT

We introduce a Monte Carlo based real-time diffusion process for shape-based analysis in volumetric data. The diffusion process is carried out by using tiny massless particles termed shapetons, which are used to capture the shape information. Initially, these shapetons are randomly distributed inside the voxels of the volume data. The shapetons are then diffused in a Monte Carlo fashion to obtain the shape information. The direction of propagation for the shapetons is monitored by the Volume Gradient Operator (VGO). This operator is known for successfully capturing the shape information and thus the shape information is well captured by the shapeton diffusion method. All the shapetons are diffused simultaneously and all the results can be monitored in real-time. We demonstrate several important applications of our approach including colon cancer detection and design of shape-based transfer functions. We also present supporting results for the applications and show that this method works well for volumes. We show that our approach can robustly extract shape-based features and thus forms the basis for improved classification and exploration of features based on shape.

Keywords

Shapeton diffusion, shape analysis, Monte Carlo, colon cancer detection, transfer-function.

1 INTRODUCTION

Much research has been undertaken to incorporate information for volume data analysis from various parameters such as voxel intensity, gradient, curvature, and size. However, incorporating shape information for volume analysis still remains a challenge. This is not the scenario in the case of manifolds, where diffusion based techniques have become popular for manifold shape analysis. A successful attempt has been made by Gurijala et al. [GWK12] in using the diffusion based method for shape-based volume analysis, wherein a modified form of heat diffusion, called cumulative heat diffuison (CHD), was introduced. Despite good results, this method cannot be adopted for real-time analysis due to the high computational cost. Precisely, the computational complexity of the heat diffusion process for discrete surface meshes is of the order $t \times n^2$, where n is the number of voxels and t is the number of time steps. In addition, the heat diffusion is carried out only between voxels and 1-ring neighboring voxels per time step and hence the number of time steps required to capture the shape information increases with the increasing number of voxels. In other words, the rate of heat flow is influenced by the resolution of the data. As a result, the diffusion based methods suffer from the problem of long running times. In order to address these challenges, in this paper, we introduce a Monte Carlo based shape analysis method for volumes which not only obtains efficient results but also provides a means of real-time shape analysis, by re-defining the diffusion process using a new set of particles, which we call shapetons. In addition, a new definition of time step is introduced.

This paper makes the following contributions. We introduce a new diffusion based shape analysis method using new particles, called shapetons. The shapetons are tiny massless particles which are diffused across the voxels of a volume, in random directions, for a predefined distance per time step, to determine the local shape information. This is the first time the diffusion particles (in our case, the shapetons) are diffused across the voxels separated by some distance, rather than just between the adjacent voxels. Our method is independent of the size of the volume; it only depends on the number of shapetons. This independence on the resolution (size) of the data is another important contribution of the paper. In addition, using probabilistic methods for shape analysis is in itself a contribution. All the shapetons can be diffused simultaneously and independent of each other. As a result, our method can run in parallel for all the shapetons. We use the GPU for implementation and the convergence of the shapetons to a stable value can be monitored in real time, thereby fa-

cilitating real-time shape analysis. To the best of our knowledge, this is the first time volume analysis based on shape with real-time monitoring of the result is being carried out, thereby achieving orders of magnitude improvement in the computational cost.

The remainder of the paper is organized as follows. Section 2 provides background information and reviews the related literature. Section 3 describes the algorithm with a detailed description of the shapeton diffusion process. We discuss how our shapeton diffusion method can robustly extract the features based on their shape information in the volume data. The influence of different parameters on the result is analyzed in Section 4. Section 5 discusses applications of our method in colon cancer detection and transfer function design and Section 6 presents the results of our method. Finally, we draw some concluding remarks along with the future work in Section 7.

2 RELATED WORK

Shape has been previously used for volume classification. Sato et al. [YSABNSK00] have proposed a volume classification based on shape where they detect pre-defined shapes such as edge lines and blobs by measuring the multi-scale responses to 3D filters. Skeleton based approaches were extensively used to study shapes and for shape based volume visualization. Hilaga et al. [HSKK01] have used skeletons for shape matching and volume visualization. Pizer et al. [PGJA03] have proposed a framework of stable medial representation for segmentation of objects, registration and statistical 3D shape analysis. Several other attempts using skeletons for shape-based volume classification were conducted by Correa et al. [CS05] and Reniers et al. [RJT08]. Motivated by these ideas, Praßni et al. [PRMH10] have presented a shape-based transfer function using the curve-skeleton of the volumetric structure. However, in all these works, the shape has been pre-defined such as blobs, surfaces and tubes. In contrast, we enforce no shape restrictions. All similar shapes, irrespective of orientation and scaling are recognised and at the same time distinguished from other shapes.

In volumes, the diffusion methods have been majorly used in the form of photon diffusion in the volume rendering pipeline [Jen96]. Apart from this, diffusion based models have also been used to visualize fire [SF95], air pollution [Wan13], and rendering depth of field effects [KB07]. None of these diffusion based approaches have been used for shape analysis. Diffusion based methods have been used extensively for shape analysis in manifolds [ASC11, BK10, OMMG10, SOG09, VBCG10]. However, these methods cannot be directly extended to volumes for shape analysis due to the huge computational cost. The only attempt to perform volume analysis based on shape was made very recently by Gurijala et al. [GWK12] who introduced a cumulative heat diffusion approach. Despite the novelty, the method still has a large computational cost and the shape analysis cannot be monitored in real-time. Using our shapeton diffusion approach, we are able to not only peform shape-based volume analysis but also monitor the analysis in real-time.

Monte Carlo methods are not new to volume graphics and visualization [AK90, BSS94, PM93]. They have been largely used for photorealistic rendering (photon mapping) [DEJ$^+$99, Jen96, JC98] and ray tracing (rendering volumetric caustics and shadows) [JLD99, LW96, PKK00]. Unfortunately, most of these methods have high computational cost. To solve this, several variations of Monte Carlo photon diffusion approximation methods have been proposed for various rendering applications [DJ05, JMLH01, Sta95]. All these Monte Carlo based photon diffusion methods are a combination of a diffusion model and Monte Carlo methods ala our technique. A GPU-based Monte Carlo volume rendering approach including scattering, ambient occlusion has been proposed by Salama [Sal07]. However, none of these methods focus on shape analysis in volumes. Ours is the first time a Monte Carlo based method using GPU has been developed for shape based volume analysis, thereby facilitating a real-time monitoring of the shape information.

3 ALGORITHM

The shapeton diffusion process efficiently captures the shape information in volumes and in addition facilitates a real time monitoring of this information. The diffusion particles, the shapetons, are able to capture the majority of the shape information and hence the name shapetons. Initially, these shapetons are randomly distributed inside the data. The primary idea of our approach is that each shapeton is diffused based on the local shape information in a probabilistic manner. The probability that a shapeton moves in a particular direction is based on how much the region in that direction contributes to the shape information. In continuous space, generally the shape information around each shapeton can be represented in the form of an uneven distribution. This is because the local shape information around the shapeton is not uniform (varies depending on the data). The area of this shape distribution would give a measure of the shape information obtained around the shapeton. A random number is used to select a fraction of the area. This fractional area indicates the shape information obtained in that direction and in turn the probability for the shapeton to move in that direction. In other words, the probability of shapeton diffusion is based on the ratio of the area of a sub-region to the area of the total shape distribution. The difference between our method and previous diffusion based

methods such as the cumulative heat diffusion (CHD) is that, ours is a particle-based (shapetons) diffusion process while the latter is not. During the diffusion process the shapetons are moved inside the volume, across the voxels, for a pre-defined distance in each time step. As a result, the shapetons have the freedom to move anywhere inside the volume and not just between the 1-ring neighboring voxels. Therefore, the rate of shapeton diffusion is not affected by the resolution of the data and is independent of the size of the data. In the remainder of the paper, please note that all the pre-defined distance values are chosen by considering a $[0,1]$ normalized space of the volume data. Hence, the distance value will always lie in the interval $[0,1]$. Initially, all

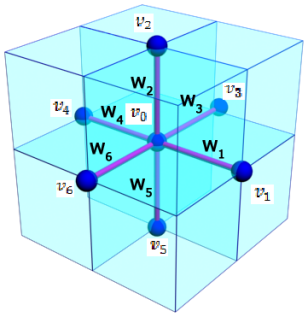

Figure 1: $v_1, v_2, v_3, v_4, v_5, v_6$ are the 1-ring neighboring voxels of the source voxel v_0 and w_1, w_2, w_3, w_4, w_5 and w_6 are the corresponding edge weights respectively.

the shapetons are randomly distributed inside the voxels. The initial distribution of the shapetons does not influence the final result. Only the steady state result is considered for shape analysis. The steady state result will smooth out the differences and is not affected by the initialization of the shapetons. We will discuss in detail about the steady state later. The shapetons are diffused inside the volume based on the local shape information. In order to describe the direction along which the shapetons travel in each time step, two angles are used, namely the longitudinal angle and the latitudinal angle. We now describe the elaborate process of shapeton diffusion in detail. In general, any voxel is surrounded by six adjacent voxels in a volume. Thus, for any shapeton s inside a voxel (say v_0), there are six adjacent voxels (say v_1, v_2, v_3, v_4, v_5 and v_6).

The edge weights w_1, w_2, w_3, w_4, w_5 and w_6 between the voxel v_0 and its adjacent voxels, as shown in the Figure 1, are determined using the VGO [GWK12], defined by Equation 1. This VGO captures the local shape information of the volume. There is a parameter p in the VGO definition that influences the final result. We discuss the effect of the parameter p in Section 4.5. For $i \in \{1,2,3,4,5,6\}$:

$$w_i = VGO(v_0, v_i) = \Delta(v_0, v_i) + F_v(v_0, v_i) \qquad (1)$$

where Δ is the Laplace-Beltrami Operator (LBO) and F_v is a data-driven operator:

$$F_v(v_0, v_i) = 1 - p \cdot h_g(v_0, v_i) \qquad (2)$$

where h_g is the half gradient and p is a user defined value. The half gradient h_g of the voxel v_0 is given by:

$$h_g(v_0, v_i) = |\frac{I(v_i) - I(v_0)}{res}| \qquad (3)$$

where I gives the intensity of the corresponding voxel, res is the size of the voxel which accounts for the distance between the two voxels under consideration.

We use these six edge weights to create a shape distribution diagram around the shapeton, as shown in Figure 2. This shape distribution accounts for the shape information around the voxel v_0 (the shapeton is inside this voxel) and is used to determine the direction of shapeton diffusion in a probabilistic manner. The six weights form eight regions where each region represents an octant of a sphere. We call this octant of the sphere octavusphere (derived from Latin). Therefore, the six weights form eight octavuspherical regions where sets of three weights form a single octavuspherical region, as shown in Figure 2. In spherical coordinates we normally need two angles (say θ and ϕ) to describe the direction of shapeton propagation. The angle θ is measured with respect to the x-axis on the $x-y$ plane and the angle ϕ is measured with respect to the y-axis on the $y-z$ plane. In geographical terms, we refer to the angle θ as the longitudinal angle and the angle ϕ as the latitudinal angle.

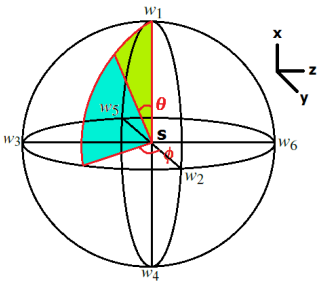

Figure 2: The shape distribution around the shapeton s shown using the edge weights. The probabilistically estimated angles ϕ and θ define the direction of the shapeton propagation.

Since we have to determine two angles probabilistically, namely θ (longitude) and ϕ (latitude), two random numbers are drawn, one for each of them. We do it in a step-by-step manner. First, the value of the angle ϕ is determined by employing the first random number. Fixing this value of ϕ, the value of the angle θ is then estimated by employing the second random number. In a given octavuspherical region both ϕ and θ vary between 0 and $\frac{\pi}{2}$. The probability of the shapeton

diffusion should take into account the shape information around it, which is indicated by the volume of the octavuspherical region enclosed by the edge weights. In other words, the probability of the shapeton to move in a certain octavusphere is based on the ratios of the volumes of the octavuspheres to the whole volume. By employing the first random number over the volumes of the octavuspherical regions, a particular octavusphere region is selected and the corresponding value of ϕ is estimated. This angle ϕ splits the selected octavuspherical region into two sub-regions, which are separated by a sector shown by the green and blue regions in Figure 2. By employing a second random number over the area of this sector the final value of θ is estimated. More details about the steps involved in calculating the longitude and latitude for shapeton propagation are provided in Appendix 4.

Now that we have evaluated both ϕ and θ, we have the final direction for the shapeton to move. Once the direction of propagation for the shapeton is determined, the shapeton is moved in that direction for a pre-defined distance. This accounts for one time step of the shapeton. This process is performed for all the shapetons independently and simultaneously. After each time step, all the steps described above are repeated to calculate the new direction for the shapetons to diffuse. After each time step, the number of shapetons inside each voxel is summed up to get the accumulated density of shapetons. For example, let $s_{t-1}(i)$ be the accumulated shapeton density on a vertex i before the t_{th} time step and c_t be the number of shapetons that move onto that vertex from its neighboring vertices during the t_{th} time step. Then, the new accumulated shapeton density $s_t(i)$ on that vertex is:

$$s_t(i) = s_{t-1}(i) + c_t \tag{4}$$

The value of c_t will either be positive or zero and never negative since we only consider the number of shapetons that accumulate in each of the voxels after each time step and not the number of shapetons that diffuse away from the voxels. Note that no new shapetons are added at any stage of the algorithm and the number of shapetons used for diffusion is always constant. Only the shapetons diffuse inside the volume and based on which voxel each of the shapetons are present after every time step, the corresponding accumulated shapeton density of those voxels are updated. The accumulated number of shapetons in each voxel indicates the probability of the shapetons to appear at that location. For all the voxels corresponding to objects of similar shape, the shapetons have a similar probability to visit them. Hence, the number of shapetons within each voxel would be the same for all voxels corresponding to objects of similar shape. The diffusion of shapetons in volumes is influenced by the VGO which incorporates the local shape information. Thus, the shapetons capture the shape information along their path of diffusion and the accumulated number of the shapetons inside the voxels quantifies the shape information obtained.

4 ANALYSIS

The shapeton diffusion process is an efficient method in classifying different objects based on their shape. The shape information is obtained irrespective of the size and deformation of the objects. However, the amount of shape information obtained is influenced by a number of parameters such as the number of shapetons, the value of the pre-defined distance, and the value of p. In the remainder of the paper, for all the results, the rendering is based on the accumulated number of shapetons in the voxels for a given number of time steps and the colors are assigned such that a higher shapeton count is shown in red and the color changes from red to blue with the decrease in the shapeton count.

4.1 Steady State

Like any Monte Carlo method, the probability of the shapetons to take a particular path increases as we increase the number of shapetons and hence the rate of accumulation of shapetons at a particular feature increases. Thus, the shape information is obtained much faster in terms of the number of iterations with the increase in the number of shapetons. If the number of shapetons is reduced, it takes more iterations to capture a specific feature, which otherwise would have taken fewer iterations using more shapetons. However, there is a tradeoff. Though the number of iterations decreases, the time taken for each iteration (time step) increases with the increase in the number of shapetons.

We say that the shapeton diffusion process has reached a steady state if the rate of change of the accumulated shapeton density on all the voxels is uniform. For this, we check if the rate of change of the accumulated shapeton density on all the voxels after every time step ($\Delta t = 1$) is below a threshold value as follows:

$$\Delta s(t) = \sum_{i \in V} (s_t(i) - s_{t-1}(i))^2 \leq \varepsilon \tag{5}$$

where $\Delta s(t)$ denotes the rate of change in the accumulated shapeton density for all the voxels after t time steps, V denotes the number of voxels in the volume, $s_t(i)$ and $s_{t-1}(i)$ are the accumulated shapeton densities on voxel i after t and $t-1$ time steps respectively and ε is the threshold value. In all our datasets, we choose the threshold value to be 0.05. This threshold value chosen is not an accurate estimation and is chosen experimentally by observing the shapeton diffusion process on several datasets. As future work, we plan on finding a way to provide a more accurate estimate of the

threshold value that will be dependent on the dataset. We check if the condition in Equation 5 is satisfied continuously in atleast 90% of the last 50 time steps. The 10% leverage is given to account for some unexpected changes caused due to the probabilistic movement of the shapetons. The number of time steps after which all these requirements are satisfied is chosen to be the point where a steady state is reached.

4.2 Distance Value

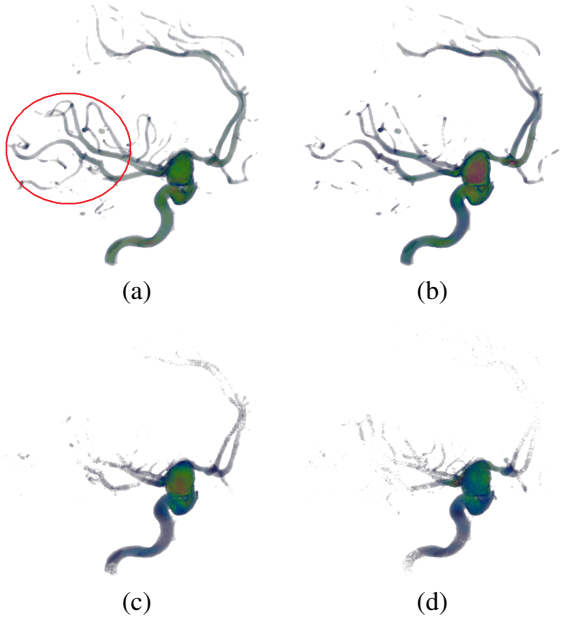

Figure 3: Effect of the different distance values on the aneurysm volume data using 400 time steps. Smaller features such as the narrow blood vessels (shown in the red circle) are captured using small distance values of 0.001 in (a) and 0.005 in (b) which are absent when larger distance values of 0.01 in (c) and 0.05 in (d) are used.

When a shapeton travels a pre-defined distance (defined by the user), it is said to complete one time step or iteration of the diffusion process. This distance value also affects the diffusion process of the shapetons and the shape information captured. When we use a large distance value, the shapetons travel a larger distance in one time step. Thus, if we increase the distance value the diffusion process converges faster in terms of the number of time steps when compared to a lower distance value. The smaller distance values cause the shapetons to move slowly, thereby resulting in more time steps needed to capture the global shape. However, the catch here is that we cannot obtain the local features using a large distance value because most of the shapetons will travel over the smaller features missing them completely. Smaller distance values are useful in obtaining and analyzing local features. Therefore, the distance value is an indication of the shape information obtained at different scales of the data. Intricate local shape details are obtained by using a smaller distance value, while global shape information is obtained using a higher distance value (with a smaller number of time steps). It is not that the smaller distance value is unable to capture the global shape information, it is just that it takes more time steps to obtain the global shape information using a smaller distance value. On the contrary, a higher distance value is unable to obtain the local features despite using more time steps.

Figure 3 shows the results of the shapeton diffusion on the aneurysm dataset using different distance values for the same number of 400 time steps. Figure 3(a) shows the result for a distance value of 0.001; Figure 3(b) shows it for a distance value of 0.005; Figure 3(c) shows it for a distance value of 0.01, and Figure 3(d) shows the result for a distance value of 0.05. For small distance values even the smaller features such as the narrow blood vessels (shown in the red circle) are captured. As the distance value is increased, only the relatively larger features such as the aneurysm blob are captured by the shapetons. The smaller features such as the narrow vessels are missing in Figures 3 (c) and (d), where a higher distance value is used.

4.3 Shape Classification

We now show that our shapeton diffusion method is indeed successful in classifying different shapes. The shapetons are diffused based on the VGO in volumes, which captures the shape information. Hence, the probability of a shapeton to go in a particular path is influenced by the shape information. The accumulated number of shapetons per voxel in a shape such as a cube would be different from a shape such as a sphere since both of them have different shape and thus bear different probabilities for the shapetons to capture them.

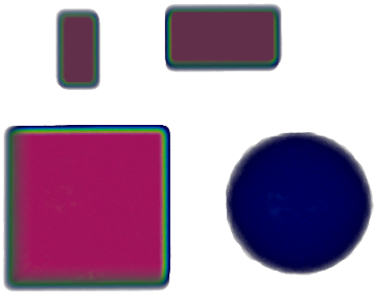

Figure 4: Shape classification capability of the shapeton diffusion approach shown using a synthetic data consisting of a cube, two cuboids of different size and orientation and a sphere.

We use a synthetic data consisting of a cube, two cuboids of different size and orientation and a sphere to confirm this. Figure 4 shows the result of using the shapeton diffusion method on the synthetic data. We consider a large number of 2500 time steps to make

sure that a stable state is reached. In each time step, the shapeton was moved by a distance of 0.01. We can clearly see from Figure 4 that all the shapes have been identified and distinguished successfully (shown by the different colors). The colors are assigned based on the number of shapetons accumulated. The shapeton propagation is based on the shape information (VGO) and hence the number of shapetons accumulated per voxel is the same in similar shaped objects. This fact can be observed in Figure 4 where both cuboids have the same color. In addition, the color of the cube is almost similar to that of cuboids indicating that they have almost similar shape. The cube and the sphere have also been classified as different shapes, thus asserting that the shapeton diffusion method serves as a powerful tool in finding objects with similar shape and distinguishing them from objects with other shape. An important observation that can be made from Figure 4 is that both cuboids have been identified as similar shape irrespective of their size and orientation. This further confirms that our method can recognize different shapes independent of their size and orientation.

4.4 Invariance to Deformations

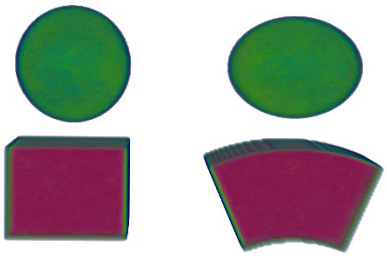

Figure 5: Objects of similar shape identified successfully irrespective of their deformations.

The shapeton diffusion method displays some lucrative properties such as invariance to deformations. We generated a synthetic data to establish this property. The synthetic data consists of a cuboid, a deformed cuboid, a sphere and a deformed sphere. Figure 5 shows the result of the shapeton diffusion on this synthetic data. Again the diffusion process is carried out for a large number of time steps to ensure a stable state is reached and all the objects in the volume data are obtained.

You can observe that although the cuboid has been deformed, the number of shapetons accumulated per voxel in both the cuboid and its deformed version are the same and hence both have similar color. Likewise, the sphere and its deformed version have similar color. The sphere and the cuboid have also been distinguished from each other. We used 1000 shapetons for 2500 time steps to obtain the results. The results in Figure 5 show that the shapeton diffusion method is successful in identifying objects of similar shape though they have been deformed, thus proving that it is invariant to deformation.

4.5 Effect of p

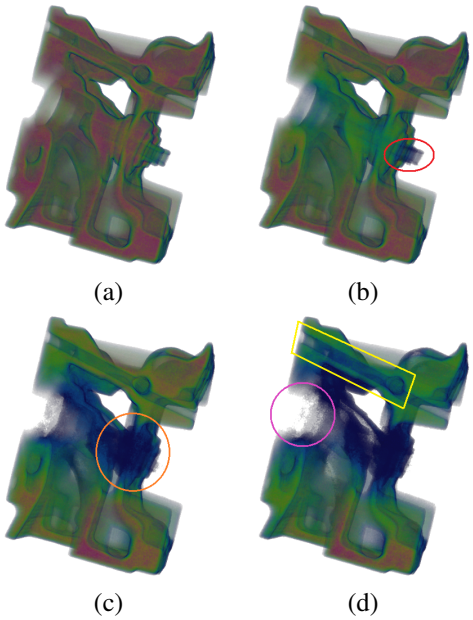

Figure 6: Comparison of choosing different values for p. (a), (b), (c) and (d) are the results obtained by choosing p = 4, 9, 15 and 20, respectively, on the engine dataset for 1300 time steps. Internal parts such as the pipe (shown in the red ellipse), the outer rim around the pipe (shown in the orange circle) and the beam (shown in the yellow box) are captured in (b), (c) and (d), respectively. For large values of p in (d) some of the global shape information is missing (shown in the pink circle).

The direction of shapeton propagation is guided by the VGO. VGO has a parameter p which influences the result obtained. p is a user defined parameter that is used to decide the boundaries of the objects in a given volume data. The clarity of the boundary determines how clearly the different shapes are identified. The parameter p gives the user extra flexibility in deciding the object boundaries. A large p value would enhance the local shape differences within an object and hence result in more sub-objects. Therefore, by increasing the value of p the local internal objects within an object can be obtained. However, we tend to lose some of the global shape information for larger values of p. Thus, the final results obtained might vary both locally and globally for different values of p based on how well the objects are distinguished and how sharp the features are. All these effects of p are shown experimentally using the engine data in Figure 6.

Figure 6 shows the result of choosing different values of p on the engine dataset. Figures 6(a), (b), (c) and (d) show the result when p = 4, 9, 15 and 20, respectively for 1300 time steps with a pre-defined distance

of 0.05. We can observe that different parts of the engine are captured by using different values of p. In Figure 6(b) where $p = 9$, the internal pipe (shown in the red ellipse) is separated which was not when $p = 4$ in Figure 6(a). Similarly, when $p = 15$ in Figure 6(c) the outer rim around the pipe (shown in the orange circle) is captured. Finally, when $p = 20$ in Figure 6(d) the beam of the engine (shown in the yellow box) is captured. We can see that by increasing the value of p more internal parts of the engine are captured as the local shape differences between these parts are enhanced. However, some of the global shape information is missing (shown in the pink circle) in Figure 6(d). This is because a high value of p divides the same object into much smaller sub-parts and because the pre-defined distance used was relatively high, these smaller sub-parts are not captured. The same is the reason why the internal pipe from Figure 6(b) is missing in Figures 6(c) and (d). In this way, different parts of the engine based on their shape can be obtained and analyzed using different values of p. This facilitates a better analysis and understanding of the data. As the convergence of shapetons can be monitored in real time, even though the value of p is changed, the new result can be obtained very fast. Thus, based on what features the user wishes to focus on and what features the user wants to analyze, different values of p can be selected.

5 APPLICATIONS

5.1 Transfer Function Design in Volumes

The shapetons accumulate all the shape information over different time steps while diffusing inside the volume. This information can be used to design a shape-based transfer function. The user can assign different colors and opacities to the final accumulated shapeton count, which forms a 1-D transfer function based on the shape information.

Figure 7 shows a volume rendered image of a CT chest dataset with a transfer function designed using the shape information obtained by our shapeton diffusion method. We were able to classify different parts of the data, such as the rib bones (shown in red), the sternum (shown in dark green), the clavicle bones (shown in magenta), the soapula (shown in fluorescent green), and small bones of the spinal cord (shown in blue) based on the shape information. Figure 7 shows all the segmented parts of the CT chest data by using our transfer function. All the ribs have similar curved shape and hence have been classified as the same shape indicated by the same color. Even the small but important part named xiphoid (greyish blue shown in the black circle), which is present at the tip of the sternum has been classified by the shape-based transfer function. The number of shapetons used was 65000 with a distance value of 0.05. The diffusion process was carried out for 1600 time steps, for a total time of 3.10 sec.

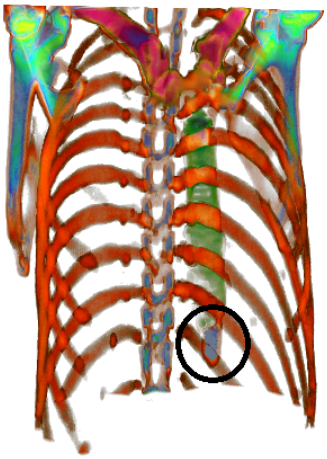

Figure 7: Volume rendering with the shape-based transfer function on the CT chest dataset. The rib bones (red), the sternum (dark green), the clavicle bones (magenta) and the soapula (fluorescent green) are obtained. The small bones of the spinal cord (blue), xiphoid (greyish blue in the black circle) - a small part present at the tip of the sternum are also classified.

5.2 Colon Cancer Detection

Colorectal cancer is the second leading cause of cancer related deaths in United States. Polyps are the precursors of colorectal cancer. Polyps are small protrusions of the tissue that grow out of the walls of the colon. Early detection and removal of these polyps is important for preventing colon cancer. We used our shapeton diffusion approach to detect the polyps on the colon surface, obtained from a CT scan of the patient's abdomen for virtual colonoscopy (VC) [HMK+97].

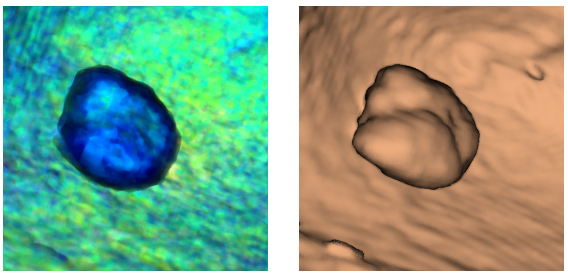

(a) (b)

Figure 8: Polyp detection inside the colon using the shapeton diffusion method. (a) Polyp (shown in blue) detected using our approach; (b) Volume rendering of the corresponding location inside the colon confirming the presence of the polyp.

We used real volumetric colon data from VC to show the effectiveness of the shapeton diffusion process in polyp detection. The volumetric colon is electronically cleansed CT data. Figure 8 shows the result of the polyp detection using our shapeton diffusion method on the real colon data. Figure 8(a) shows the result obtained by our method and Figure 8(b) shows the volume ren-

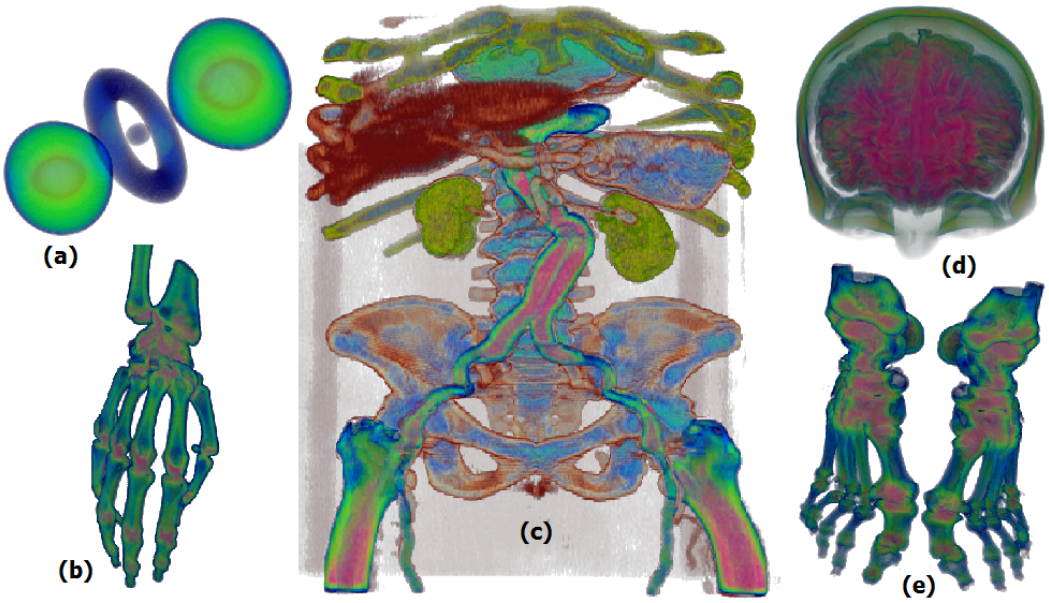

Figure 9: Classifying objects based on their shape using our shapeton diffusion approach on (a) hydrogen atom, (b) visible female hand, (c) CT abdomen, (d) MRI head, and (e) visible female feet volumetric datasets.

dering result of the corresponding location of the polyp inside the colon. Since polyps have a blob-like shape, different from the shape of the colon walls, we were able to successfully detect the polyps using our method. Figure 8(a) shows one such polyp (shown in blue) detected. We confirmed the position of the polyp by examining the corresponding location inside the colon volume data. This result can be seen in Figure 8(b). It took just 4000 time steps using 65000 shapetons to achieve this result. The p value was chosen to be 15. The reason to choose a high value for p is to get a clear boundary of the polyps. Since a smaller scale is needed for the polyp detection, a low distance value of 0.005 was chosen. The total time taken was 5.44 sec.

6 RESULTS

We used several datasets to demonstrate the efficiency of our method. Figures 9 (a)-(e) show the object classificaiton capability of our approach based on the shape information for hydrogen atom, visible female hand, CT abdomen, MRI brain and visible female feet volumetric datasets, respectively. In Figure 9(a) both the orbitals of similar shape are clearly distinguished from the nucleus (center) and the orbit (around the nucleus) in a hydrogen atom as inidicated by different colors. In Figure 9(c), the shape-based volume exploration of the CT abdomen reveals various organs such as the kidneys, liver, pancreas, and vital parts such as the aortic vessel, spinal cord and pelvic bones using 260000 shapetons and a pre-defined distance of 0.01. All the internal organs have different shapes and by virtue of our method, they have been identified successfully. Furthermore, it has just taken only 2.13 sec using 2600 time steps to obtain this result. In Figure 9(d), we are able to separate the brain from the cranium and eye sockets in the MRI head data, using the shape-based transfer function designed by our approach. We used 65000 shapetons for a pre-defined distance value of 0.01 and 4160 time steps which accounted for a total time of 2.82 sec. Figures 9 (b) and (e) show that the bones and the joints between the bones are identified in the visible female hand and feet data, respectively. While we used 65000 shapetons and a pre-defined distance of 0.01 in both the cases, the number of time steps were 460 and 420 with a total time of 0.34 sec and 0.27 sec for the visible female hand and feet, respectively.

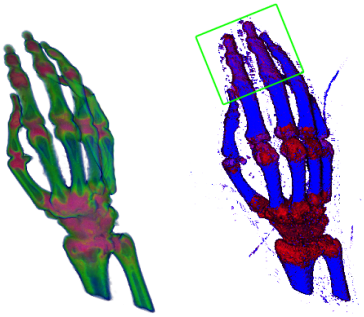

(a) (b)

Figure 10: Visual comparison of the results obtained for the visible female hand dataset using (a) Our shapeton diffusion method and (b) The cumulative heat diffusion method.

We compared our approach with the cumulative heat diffusion (CHD) approach [GWK12], in terms of the running time per iteration and the number of time steps required to obtain visually similar or even better results. Table in Appendix 5 shows the comparison re-

sults using different volume datasets. For the sake of completion, we also provide a visual comparison of the results obtained by using our method with that of the results obtained using the CHD method using the visible female hand dataset (see Figure 10). Figure 10(a) shows the results obtained using the shapeton diffusion approach, while Figure 10(b) shows the result obtained by using the CHD method. In Figure 10(b), 1000 time steps were considered while in Figure 10(a) only 460 time steps were considered for a distance value of 0.01. Since we wanted to capture the local features, a smaller distance value was used. The same p value of 10 was used in both the cases. We can clearly observe that visually better results were obtained using our method compared to the CHD method. We can also see that a better distinction of shapes was obtained using our method even in very local regions, as indicated by the region in the green box in Figure 10(b). The joints have been clearly distinguished from the hand bones. Furthermore, the result was obtained in much less time compared to the CHD approach, further emphasizing the superiority of our method.

7 CONCLUSION AND FUTURE WORK

The main contribution of this paper is the real time shape analysis method in volumes using a Monte Carlo approach. Tiny massless particles, called shapetons, are diffused based on the VGO in a Monte Carlo manner. In addition, a new definition for the time step using a pre-defined distance is introduced. Unlike the conventional diffusion based methods, this method is independent of the size and resolution of the data. The final accumulated shapeton count after each time step would capture the shape information and helps in analyzing the data based on shape. The diffusion process can be monitored in real time and this facilitates a real time shape analysis of different features until a convergence state is reached. Furthermore, we discuss the properties of our method by presenting results using simple as well as complex datasets. Important applications of our method to colon cancer detection and transfer-function design have also been discussed, along with supporting results.

The results obtained using our method are influenced by many parameters such as the number of shapetons, the distance value, the number of time steps t, and the value of p. As discussed earlier, there is an optimum value for the number of shapetons used after which the time taken to obtain the results increases even though the number of shapetons is increased. Similarly, the time step t and the value of p have optimum values to obtain the best results based on the dataset used. As part of our future work, we plan to focus on finding a way to automatically decide the optimum values for all the parameters in order to obtain the best results.

8 REFERENCES

[AK90] James Arvo and David Kirk. Particle transport and image synthesis. *SIGGRAPH Computer Graphics*, 24(4):63–66, September 1990.

[ASC11] Mathieu Aubry, Ulrich Schlickewei, and Daniel Cremers. The wave kernel signature: A quantum mechanical approach to shape analysis. *ICCV Workshops*, pages 1626–1633, 2011.

[BK10] Michael M. Bronstein and Iasonas Kokkinos. Scale-invariant heat kernel signatures for non-rigid shape recognition. *CVPR*, pages 1704–1711, 2010.

[BSS94] P. Blasi, B. L. Saec, and C. Schlick. An importance driven monte-carlo solution to the global illumination problem. *Proceedings of the Eurographics Workshop on Rendering*, pages 173–183, 1994.

[CS05] Carlos D. Correa and Deborah Silver. Dataset traversal with motion-controlled transfer functions. *IEEE Visualization*, pages 359 – 366, October 2005.

[DEJ+99] Julie Dorsey, Alan Edelman, Henrik Wann Jensen, Justin Legakis, and Hans Køhling Pedersen. Modeling and rendering of weathered stone. *SIGGRAPH*, pages 225–234, 1999.

[DJ05] Craig Donner and Henrik Wann Jensen. Light diffusion in multi-layered translucent materials. *ACM Transactions on Graphics*, 24(3):1032–1039, July 2005.

[GWK12] Krishna Chaitanya Gurijala, Lei Wang, and Arie E. Kaufman. Cumulative heat diffusion using volume gradient operator for volume analysis. *IEEE Transactions on Visualization and Computer Graphics*, 18(12):2069–2077, Dec 2012.

[HMK+97] Lichan Hong, Shigeru Muraki, Arie E. Kaufman, Dirk Bartz, and Taosong He. Virtual voyage: interactive navigation in the human colon. *SIGGRAPH*, pages 27–34, 1997.

[HSKK01] Masaki Hilaga, Yoshihisa Shinagawa, Taku Kohmura, and Tosiyasu L. Kunii. Topology matching for fully automatic similarity estimation of 3D shapes. *SIGGRAPH*, pages 203–212, 2001.

[JC98] Henrik Wann Jensen and Per H. Christensen. Efficient simulation of light transport in scences with participating media using photon maps. *SIGGRAPH*, pages 311–320, 1998.

[Jen96] Henrik Wann Jensen. Global illumination using photon maps. *Proceedings of the Eurographics Workshop on Rendering Techniques*, pages 21–30, 1996.

[JLD99] Henrik Wann Jensen, Justin Legakis, and Julie Dorsey. Rendering of wet materials. *Proceedings of the Eurographics Workshop on Rendering Techniques*, pages 273–282, 1999.

[JMLH01] Henrik Wann Jensen, Stephen R. Marschner, Marc Levoy, and Pat Hanrahan. A practical model for subsurface light transport. *SIGGRAPH*, pages 511–518, 2001.

[KB07] Todd J. Kosloff and Brian A. Barsky. An algorithm for rendering generalized depth of field effects based on simulated heat diffusion. *Proceedings of the International Conference on Computational Science and its Applications*, pages 1124–1140, 2007.

[LW96] Eric P. Lafortune and Yves D. Willems. Rendering participating media with bidirectional path tracing. *Proceedings of the Eurographics Workshop on Rendering Techniques '96*, pages 91–100, 1996.

[OMMG10] Maks Ovsjanikov, Quentin Mérigot, Facundo Mémoli, and Leonidas J. Guibas. One point isometric matching with the heat kernel. *Computer Graphics Forum*, 29(5):1555–1564, 2010.

[PGJA03] Stephen M. Pizer, Guido Gerig, Sarang C. Joshi, and Stephen R. Aylward. Multiscale medial shape-based analysis of image objects. *Proceedings of the IEEE*, 91(10):1670–1679, 2003.

[PKK00] Mark Pauly, Thomas Kollig, and Alexander Keller. Metropolis light transport for participating media. *Proceedings of the Eurographics Workshop on Rendering Techniques*, pages 11–22, 2000.

[PM93] S. N. Pattanaik and S. P. Mudur. Computation of global illumination in a participating medium by Monte Carlo simulation. *The Journal of Visualization and Computer Animation*, 4(3):133–152, September 1993.

[PRMH10] Jörg-Stefan Praßni, Timo Ropinski, Jörg Mensmann, and Klaus H. Hinrichs. Shape-based transfer functions for volume visualization. *IEEE Pacific Visualization Symposium*, pages 9–16, Mar 2010.

[RJT08] Dennie Reniers, Andrei Jalba, and Alexandru Telea. Robust classification and analysis of anatomical surfaces using 3D skeletons. *VCBM*, pages 61–68, 2008.

[Sal07] Christof Rezk Salama. GPU-based Monte Carlo volume raycasting. *Proceedings of the 15th Pacific Conference on Computer Graphics and Applications*, pages 411–414, 2007.

[SF95] Jos Stam and Eugene Fiume. Depicting fire and other gaseous phenomena using diffusion processes. *SIGGRAPH*, pages 129–136, 1995.

[SOG09] Jian Sun, Maks Ovsjanikov, and Leonidas J. Guibas. A concise and provably informative multi-scale signature based on heat diffusion. *Computer Graphics Forum*, 28(5):1383–1392, 2009.

[Sta95] Jos Stam. Multiple scattering as a diffusion process. *Proceedings of the Eurographics Workshop on Rendering Techniques*, pages 41–50, 1995.

[VBCG10] Amir Vaxman, Mirela Ben-Chen, and Craig Gotsman. A multi-resolution approach to heat kernels on discrete surfaces. *ACM Transactions on Graphics*, 29:121:1–121:10, July 2010.

[Wan13] Lei Wang. Research of air pollution dispersion visualization based on GPU and volume rendering. *Proceedings of the 2nd International Conference On Systems Engineering and Modeling (ICSEM)*, 2013.

[YSABNSK00] C.-F. Westin Y. Sato, S. Nakajima A. Bhalerao, S. Tamura N. Shiraga, and R. Kikinis. Tissue classification based on 3D local intensity structure for volume rendering. *IEEE Transactions on Visualization and Computer Graphics*, 6(2):160–180, 2000.